Optimization and Evaluation of Solar Powered Electric Rickshaw

José Carlos Furtado da Veiga[1]

[1]*Instituto Superior Técnico, Universidade de Lisboa, Lisboa, Portugal*

(Dated: October 2022)

Electric vehicles are considered a viable solution to combat greenhouse gas emissions in the transport sector. However, one of the problems holding back the global adoption of electric vehicles is the limited range, leading to range anxiety. Integrated photovoltaic production in electric vehicles is a possible alternative to this problem, namely in vehicles with limited autonomy and low power. By incorporating photovoltaic technology into the vehicle's roof, the vehicle's battery storage system can be charged while driving or even when the vehicle is parked. On the other hand, this technology makes it possible to undersize batteries, resulting in direct savings in the capital investment in the vehicle and operating costs.

Therefore, the main focus of the present thesis is to optimize the process of charging electric rickshaw batteries with on-board photovoltaics modules based on daily history of journeys, quantifying the techno-economic feasibility regarding the existence of a market for these vehicles. With the proposed system, it was possible to observe, on a typical sunny day in mid-season, an average supply of a supplement of 35% of the energy consumed by the vehicle. Furthermore, the economic analysis of the proposed system predicted a Return on Investment (ROI) of 185% throughout the vehicle's lifetime of 6 years.

It should be noted that, due to the seasonal nature of the vehicle, where greater consumption is expected on sunny days due to its tourist characteristics, these savings can be taken practically to the limit of a similar reduction in the energy capacity of the batteries.

Keywords: photovoltaic systems, electric vehicle, urban mobility, solar energy, electric charging.

NOTATION

BMS Battery Management System
η_{tot} efficiency of the motor
ω Angular frequency of rotation of the motor
τ torque acting on the motor
P_{wheels} power estimated at the wheels
P_{meas} power measured at the battery terminals
F_{ad} aerodynamic drag force
F_{rr} rolling resistance force
F_g gravitational force
F_{te} traction force
$v(t)$ velocity of the vehicle
ρ air density (1.225 kg/m^3)
C_d aerodynamic drag coefficient
A_f vehicle frontal area
f_r rolling resistance coefficient
g gravity acceleration constant (9.81 m/s^2)
α road angle
E_{batt} energy in the batteries
E_{wheel} energy at the wheels
E_{solar} energy out of the solar photovoltaic panels array
E_{grid} energy from the grid
T_{amb} ambient air temperature
T_{mod} temperature of the solar photovoltaic modules
G_T total solar irradiance
A_{act} active area of the solar photovoltaic panels array
λ longitude
ϕ latitude
h altitude
R_{earth} mean radius of the earth (6371 km)
Δs_{xy} horizontal distance traveled by the vehicle
g_{ratio} gear ratio of the drive shaft
D_{max} solar range extension per day
E_{rated} nominal capacity of the battery
E_{used} energy consumed in the vehicle on the trip
ROI Return on Investment
G_{inv} gain of investment
C_{inv} cost of investment
c_{mount} mounting cost
c_{inst} installation cost
c_{main} maintenance cost
i_r inflation rate
d_r discount rate
$E_{EV-nonsolar}$ energy consumption of the vehicle without the solar panels
C_{ele} electricity price
T_{life} project's lifetime
C_t cumulative cash flow at year t

I. INTRODUCTION

The transport sector has always played a pivotal role in the social-economic development of any country, still, despite significant improvements in all technological areas. This is a sector responsible for nearly a quarter of energy-related greenhouse gas emissions in the European Union. Particularly, road transport alone accounts for three quarters of these emissions, in which there is a considerable dependence on fossil fuels [1]. According to Energy Information Administration, it is of utmost importance to take immediate action in order to achieve carbon neutrality while ensuring the global average temperature rise is well below 1.5 degree by 2050, as targeted on the Paris Agreement [2]. This would requires a widespread shift from the internal combustion engine vehicles (ICEVs) into the electric vehicles (EVs), which make use of the electrical engines for propulsion. Of the EV types, the most used are battery electric vehicles because they are completely electric and emit zero tailpipe emissions [3].

While electric vehicles market have been grown exponentially, the role of powered light vehicles such as two- and three-wheelers have done indeed more so. These vehicles are often used in urban areas that travel

short distances at low speeds, taking fairly small battery packs [4]. Since they generally do not require a license to drive, they are much easier to operate and handle mainly in urban areas, making them a good candidates for electrification [5]. Despite the benefits, continuing challenges to the global acceptance of these vehicles still exist. The most prominent one is the limited driving range, leading to range anxiety. So it is necessary to create solution to solve this problem in order for mobility to occur.

A. The role of Renewable Energies

With regard to electricity generation, the emission of EVs is largely dependent on the mix of energy used to produce the electricity they consume. In that regard, the full environmental benefits of EVs can only be achieved when they are powered by electricity systems with a great share of renewable energy sources. Because of this, the attention of the world has been turning to renewable energies. Among these, the widespread use of photovoltaic energy, which is a free, sustainable, renewable, and clean source, has grown exponentially and is considered the third largest renewable energy in terms of capacity and energy generation [6]. To sustain this growth, from an economic perspective, such developments are due to a significant drop of about 82% in the global average price of solar photovoltaic module in the last decade [7].

Photovoltaic energy can provide clean energy to the electric vehicles through several ways. The most widely and inexpensive is to integrate solar photovoltaic energy directly on the vehicle's roof so that additional energy can be generated, thus enabling the vehicle's battery to be charged while driving or even when the vehicle is parked [8–11]. On the other hand, this approach makes it possible to undersize the batteries, resulting in direct savings in capital investment in the vehicle and operating costs.

B. Electric Rickshaw

Electric rickshaw are three-wheelers electric vehicles known by their varied names, being the most famous tuk-tuk. These three-wheelers are extensively used in Asian countries where they operate as taxi services and tourist vehicles, as well as private and cargo transport. In recent years, these vehicles have been arriving in Europe, particularly in Lisbon, they are seen to making tours in the city and are considered as the main mode of transport by tourists to explore the city quickly and comfortably, thereby contributing to the touristic ecosystem of the city [12]. However, because of its great advantages in contributing to the Portugal's economy, a very few studies focused on them were found in the literature. A study using real-world data was found to estimate its consumption [13]. Another study was found that focused on the design of a solar rickshaw in India [8]. However, no studies on the optimization and evaluation of this vehicle with the solar energy supplement were found using real-world data, which is the approach of this work.

C. Objectives

The focus of the present work, thus is to optimize the process of charging electric rickshaw batteries with onboard photovoltaic energy, quantifying its benefits based on daily history of trips. With this in mind, this work was divided into 3 main parts. First, the solar rickshaw was constructed. This involved the construction of the supporting equipment in order to fix the solar panels on the vehicle's rooftop.

Then a data acquisition system was built in order to collect and acquire important variables during vehicle trips from different sensors located inside the vehicle. In general, data regarding the solar photovoltaic panels production are acquired from the Current Meter (PZEM), and information about battery pack will be collected from a Battery Management System (BMS), following the data regarding the vehicle position from a GPS receiver using a Raspberry Pi 3.

Finally, the collected data will be analyzed and used to evaluate the real benefits of the solar panels technology in charging rickshaw batteries.

The remainder of this report is organized as follows. Section II and II A discuss the solar rickshaw electrical architecture, vehicle modeling, solar cell modeling and their environmental factors. Section III describes the construction of the solar rickshaw and the data acquisition system. Section V presents the analysis results for energy consumed, driver benefits, economic analysis, respectively. Section VII describes the new battery selected for the built solar rickshaw and Section VIII provides the conclusion of this work.

II. VEHICLE DYNAMICS MODEL

To estimate the energy consumption of the vehicle on the trips, a reliable and accurate energy prediction model is needed. A considerable amount of researchers have been done in order to estimate the energy spend for a given trip. Most of them focus on physical models that try to estimate the energy consumption by means of physical phenomena [14]. In Fig. (1) it is shown the energy flow model in a typical battery electric vehicle. It is shown that the energy harvested by the solar panels is used to charge the batteries, which in turn is used for the vehicle to move forward. During this process, there are losses in the system that need to be properly modeled. It can also be seen that the battery provides energy to the auxiliary systems, but since these are in small quantities compared to the other components, its contribution was promptly disregarded in this work.

The losses in the vehicle power-train can be modeled using Eq. (1) below, where P_{meas} is the output power measured in the battery terminals and P_{wheel} represents the input power seen at the wheels provided by the motor. This efficiency represents the joint efficiency of all the components in the vehicle power-train, that is, the controller, inverter, motor and the drive shaft [15].

$$\eta_{tot}(\omega, T_l) = \frac{P_{wheel}}{P_{meas}} \tag{1}$$

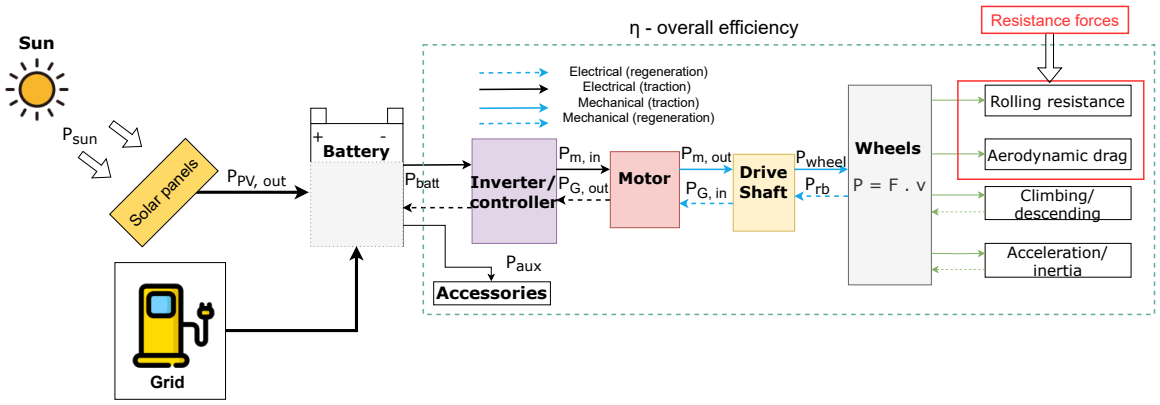

FIG. 1: Schematic representation of the sun-to-wheel and wheel-to-battery energy flows of a typical battery electric vehicle while driving; $P_{PV,out}$: PV output power; P_{bat}: battery power; P_{aux}: auxiliary power usage; $P_{M,in}$: motor input power; $P_{M,out}$: motor output power; $P_{G,in}$: generator input power, $P_{G,out}$: generator output power, P_{wheel} : power required at wheels, P_{rb}: regenerative braking power. η: represents the joint efficiency of the components in the power-train. Black lines: electrical power, blue: mechanical power, green: acting forces. Dashed lines represent flows related to regenerative braking.

To estimate this efficiency, one first needs to estimate the mechanical power seen at the wheels. One of the commonly used models is called the longitudinal dynamics model. To better understanding this model one should start by studying Fig. 2, which summarizes all the necessary resistance forces that act upon the vehicle motion; These forces are aerodynamic drag force (F_{ad}), rolling resistance force (F_{rr}) and the gravitational force (F_g). For the vehicle to overcome all these forces and move, a traction force (F_{te}) is used and applying the Newton's second law of motion, it is possible to get the main equation that governs this model and is shown in Eq. 2, where m is the vehicle mass in kg, ε_i is a factor that represents the influence of the inertia of rotating components. It depends on the speed at which the vehicle drives, but in this work it is assumed to be constant and equal to 1.05 [16]. All the aforementioned forces can be modeled according to Eq. 3.

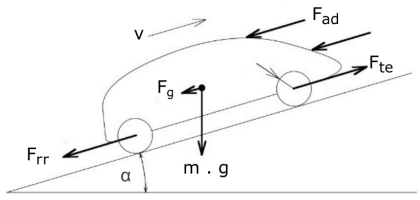

FIG. 2: Relevant forces acting on an electric vehicle moving on an inclined road considered for the typical longitudinal dynamics modeling adapted from [16].

$$m(1+\epsilon_i)\frac{dv(t)}{dt} = F_{te} - (F_{ad} + F_{rr} + F_g) \tag{2}$$

$$\begin{cases} F_{ad} = \frac{1}{2}\rho A_f C_d v^2 \\ F_{rr} = f_r mg\cos(\alpha)\left(1 + \frac{v}{Q}\right) \\ F_g = mg\sin\alpha \end{cases} \tag{3}$$

where ρ is the air density ($1.225\ kg/m^3$), C_d is the aerodynamic drag coefficient, A_f is the vehicle frontal area in m^2, f_r is the rolling resistance coefficient, g is gravitational acceleration constant ($9.81\ m/s^2$), α is the road angle in radians and Q is a parameter defined to be $160\ km/h$ to account for the small velocity dependence of the rolling resistance [16].

To find the total energy consumption (E_{wheel}) for a given trip one needs to integrate the traction force over the length traveled. The result of such integration can be seen in Eq. 3. It is of relevance to note that this energy only represents the mechanical energy provided by the motor for the vehicle to move. To find the total energy consumption of the whole system, one must subtract it from the energy generated by solar panels, as shown in Eq. 4.

$$\begin{aligned} E_{wheel} = & \underbrace{\frac{m}{2}(1+\varepsilon_i)\left[v^2(s_f) - v^2(s_i)\right]}_{\text{Kinetic energy variation}} + \\ & \underbrace{mg\left[h(s_f) - h(s_i)\right]}_{\text{Potential gravitational energy variation}} + \\ & \underbrace{f_r mg\left(\Delta s + \int_{s_i}^{s_f} v\cdot ds\right)}_{\text{Rolling energy dissipation}} + \\ & \underbrace{\frac{1}{2}\rho C_d A_f \int_{s_i}^{s_f} v^2\cdot ds}_{\text{Aerodynamic drag energy dissipation}} \end{aligned} \tag{3}$$

$$E_{batt} = \begin{cases} E_{wheel} - E_{solar}, & \text{During the day} \\ E_{grid}, & \text{Overnight} \end{cases} \tag{4}$$

A. Solar Photovoltaic Systems

Solar cells are electronic devices made out of semiconducting materials (mostly silicon) that convert incident solar radiation directly into electricity through

the photovoltaic effect. The photovoltaic effect works under the principle of charge carrier excitation under absorption of energetic photons, increasing electron density in the conduction band and holes in the valence band. Through action of the built-in potential created by the contact of doped semiconductors, the charge carriers undergo separation, creating an electric potential at the junction terminals which in turn can be used to drive a current through a circuit.

The maximum efficiency conversion for a typical silicon solar cell is 20%, so it is rare for an application in which a single solar cell is of use. Because of this, solar cells are connected in series or/and in parallel in order to obtain the desired voltage and current levels. When connecting the cells in series, the voltage level is added up, whereas if they are connected in parallel, the current is increased and the final product is called solar modules.

The performance of photovoltaic (PV) modules is in fact usually rated at Standard Test Conditions (STC), which is an industry-wide standard that defines the nominal or rated power for a given module. STC is defined as being an irradiance of 1000 W/m^2, an ambient temperature of 25° C and an air mass of 1.5 (AM 1.5) spectrum. However, these conditions generally do not represent the real working conditions of the photovoltaic module because of changes in ambient temperature, solar irradiance and wind speed, which causes the module efficiency to reduce drastically [17]. So it is of relevance to study the influence of solar panels working under varying environmental conditions in order to help optimize the performance of the modules under particular conditions. One of the parameters that significantly affect the performance of the module is the temperature of the module. The module efficiency decreases as its temperature increases. The module temperature can be estimated based on the ambient temperature (T_{amb}), module's thermal coefficient (k_T) that for the solar module used in this work is 0.0325, and the solar radiation level (G_T) in W/m^2, as shown in Eq. 5 [18].

$$T_{mod} = T_{amb} + k_T \cdot G_T \tag{5}$$

Based on this, the module efficiency can be calculated using Eq. 6, where A_{act} is the active area of the module in m^2, P_{max} is the output power of the module under NOCT provided by the manufacturer, and $\beta_T = -0.45\%/K$ is the temperature coefficient given by the module manufacturer.

$$\eta_{mod} = \frac{P_{max@NOCT}}{800 A_{act}} \cdot [1 - \beta_T (T_{mod} - T_{amb})] \tag{6}$$

III. SOLAR POWERED HYBRID RICKSHAW

The present work revolves around an electric rickshaw, commonly known as a tuk-tuk in Lisbon. In particular, the rickshaw studied is the Limo GT model manufactured by Tuk-Tuk Factory (TTF), which is a Dutch company created in 2008 with the aim of being sustainable and environmentally friendly [19] as seen in Fig. 3. This vehicle has the capacity to carry out up to 6 people including the driver and is capable of developing a maximum speed of 45 km/h. The battery pack of this vehicle consists of 24 $LiFePO_4$ lithium-ion battery cells connected in series, with a nominal voltage of 76.8 V. The rickshaw is equipped with a 7 kW three-phase AC induction motor.

FIG. 3: Picture of the **E—rickshaw Limo GT** used in this work.

A. Mounting the Solar Panels to the Roof of Rickshaw

One of the first and primary features implemented in this thesis regards the integration of solar photovoltaic panels onto the rickshaw's roof, so that additional energy can be generated, thus increasing vehicle autonomy and reducing the vehicle dependence from the grid. In this regard, the solar panels should convert incoming solar radiation into electrical energy and charge the $LiFePO_4$ battery pack as shown in previous sections. Throughout the process of turning the rickshaw into a solar rickshaw, several supporting structures were designed. The first step consisted of building a supporting structure in order to hold the solar panels together. To do this, two iron round tubes were used and then holes were drilled in order to screw the tubes to the panels and then to the isophonic claim on top of the rickshaw. The final result of the whole system can be seen in Fig. 4.

FIG. 4: Setup of the solar photovoltaic panels support.

B. Data Acquisition System

Since this is an experimental oriented thesis, a data acquisition system needed to be developed in order to

record and collected data from the multiple sensors in on-board vehicle. In general, information concerning vehicle position and its velocity was collected from GPS 18x OEM PC sensor. The information concerning the battery packs was collected from the BMS; these data contained information on the battery pack voltage, current, power, SOC etc.. And finally the information regarding the solar panels output was collected from the PZEM sensor. To acquire and save all this information into a file, a Raspberry Pi was used. The connection to the system was made using serial communication in python 3 inside the paradigm of Object-Oriented Programming (OOP) building one individual class for each acquisition sensor. The set-up used to make the acquisitions is represented in Fig. 5, in which the location of each component in the vehicle are clearly identified. It was also successfully developed an algorithm that uploaded those files into a remote server for more immediate access to the data without having to connect to the Raspberry Pi via SSH to obtain the data from anywhere and anytime in the world. The algorithm was developed in GNU Bash or shell scripting and was run on the background of the Raspberry Pi every minute.

IV. DATA TREATMENT

After the implementation of the data acquisition system, it was necessary to collect data during vehicle movement. Since we are working with experimental data, some inaccuracies should be expected, especially on the GPS-recorded data. To have a better accuracy in the model, the data was first pre-processed in order to mislead possible errors and biases associated with the data. On top of that, some relevant features that were not directly measured, which is the case of the total distance traveled and the road slope merited a special analysis and this is done in the following section.

A. Altitude Data

It is well known that the altitude data collected by the GPS is not accurate sufficient to be used in the vehicle modeling that using techniques of filtering and interpolation will be useless. The alternative of deriving the altitude data from the topological map reveals to be the best choice [13]. To correct the GPS recorded altitude data, digital map of Lisbon city was built with the help of Mapbox in Python3 using their Mapbox Terrain-RGB API, which contains elevation data encoded in a simple png image format as RGB values. It is an easy-to-use API, so obtaining the altitudes data is as straightforward as simply passing the pair of coordinate of points measured. This API gets the elevation data thanks to the realization of the Copernicus EU project, which generates its data from a weighted average of *Shuttle Radar Topography Mission (SRTM) and Advanced Spaceborne Thermal Emission and Reflection Radiometer (ASTERM)* [20]. Both datasets provide one altitude measurement for every square area of 900 m^2, which translates into one measurement for every 30 m. Figure 6 shows an example of an elevation map for the Lisbon area considered.

B. Distance Estimation

As the GPS only measures only the sequence of pairs of latitudes and longitudes along the movement, it is possible to apply trigonometric geometry to calculate the distance between two successive points. This can be achieved through equation 7, where E_{earth} represents the Earth Radius considered to be constant and equal to 6371 km, ϕ_m is the average latitude of the two successive points and $(\Delta\phi, \Delta\lambda)$ represent the variation in latitude and longitude, respectively.

$$\Delta s_{xy} = R_{earth}\sqrt{\Delta\phi^2 + (\cos\phi_m \cdot \Delta\lambda)^2} \tag{7}$$

C. Instantaneous Power Estimation

As seen the longitudinal dynamics model described in previously did not consider any losses in energy conversion in the vehicle. However, it is known that this effect has major influence in the model performance. In addition, of the components that affects the vehicles' energy consumption the most is the electric motor. The electric motor is likely to change its value significantly depending on its torque and angular velocity characteristic. The motor efficiency is commonly estimated using efficiency map as lookup table, with inputs of motor velocity and motor torque [13, 21]. Since the manufacturer did not provide no information regarding on the motor of the vehicle studied in order to base its calculation. However, using the longitudinal model described in section II, it is possible to estimate the mechanical power seen on the wheels using equation 8, where F_{te} is the traction force predicted by the longitudinal model.

$$P_{wheel} = F_{te} \cdot v \tag{8}$$

To estimate this traction force, there are some unknown variables that need to be estimated; these variables are: Acceleration and road slope. The acceleration was estimated from the variation of the velocity data and the road slope was estimated using a linear regression from the altitude and distance traveled discussed previously and estimating the slope of the line given by $\tan\alpha = \frac{\Delta h}{\Delta s_{xy}}$. Other values regarding the vehicle characteristics were measured directly from the vehicle itself; others that were difficult to measure were taken from the previous study on a similar type of vehicle [22], as shown in table II.

To estimate the efficiency map, the motor efficiency was expressed in terms of their torque and angular velocity and then computing the average efficiency for the values that fall inside the bins, as shown in equation 9, where g_{ratio} denotes the gear ratio of the drive shaft.

$$\eta_{tot}(\omega, T_l) = (T_l \cdot \omega) \cdot \frac{g_{ratio}}{P_{meas}} \tag{9}$$

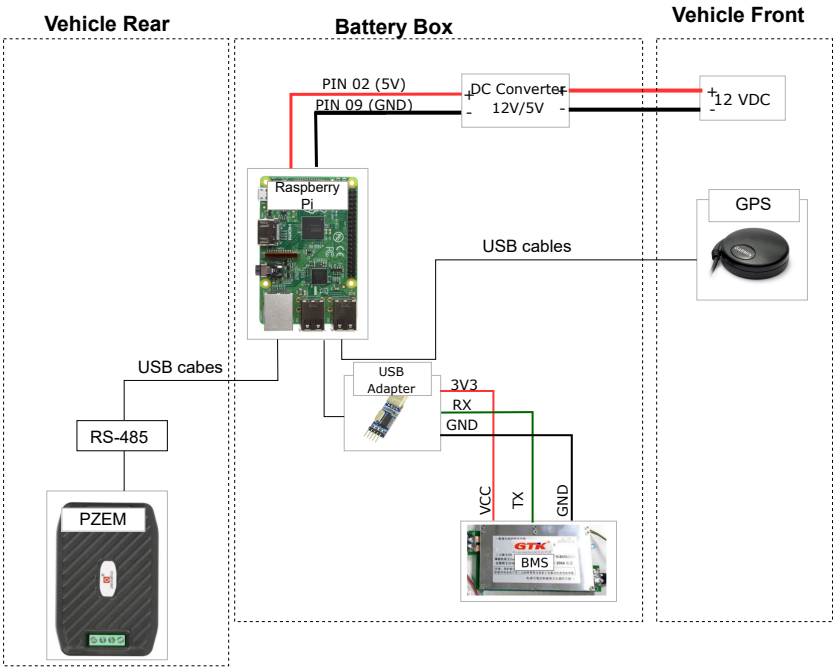

FIG. 5: Wiring diagram for connecting the GPS receiver, BMS and PZEM sensors to the Raspberry Pi.

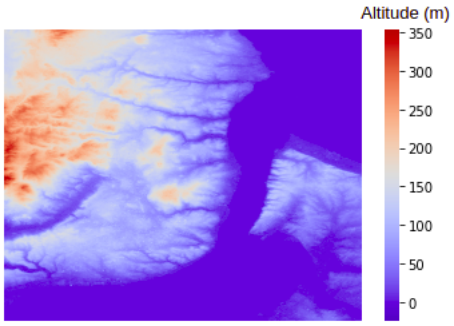

FIG. 6: Elevation map for the Lisbon area considered in the Copernicus program dataset obtained through Mapbox Terrain-RGB API.

Using that equation, it was possible to estimate the total instantaneous power of the vehicle as it travels. However, given the inaccuracy of the altitude values predicted from the topographical map it was not possible to estimate the energy consumption using this model.

V. TRIP VEHICLES' ENERGY CONSUMPTION ESTIMATION

As described previously, the estimation of the instantaneous power was not accurate enough to be used in the vehicle energy consumption on a trips, mainly because of the difficulty in correctly determining the slope of the road from the altitude data. This section aims to find a way to determine the overall vehicle consumption, but using a different approach from that used previously. In order to do that, it was derived a set of features out of the data collected that contribute to the energy consumption. The features considered are highlighted in table I.

TABLE I: Main features derived from the collected data for computing the total energy consumption of the vehicle on the trip and their respective expressions.

Term	Expression
Variation of the velocity squared	$(v_f^2 - v_i^2)$
Total distance traveled	Δs_{xy}
Altitude variation	Δh
Velocity integral	$\sum_i v_i \cdot \Delta s_i$
Velocity squared integral	$\sum_i v_i^2 \cdot \Delta s_i$

TABLE II: Suggested values for the *rickshaw Limo GT* vehicle used in the longitudinal model.

Parameter	Expected Value
Vehicle Mass (m)	893 kg
Maximum Payload	300 kg
Gear Ratio (g_{ratio})	10:1
Radius of Tire (r_{tire})	0.2895 m
Rolling Coefficient (f_r)	0.012
Drag Area (C_d A_f)	1.75 m^2

Figure 7, shows the energy balance of energy consumption for a typical sunny day, both with and without solar panels. The results reveal how solar panels can actually contribute to level-up the battery pack of the vehicle as it travels. Under the assumption that both rickshaws start at the same level of SOC, the solar rickshaw ends at 56%, while the nonsolar rickshaw SOC at 33%. Therefore, at the end of the day, the solar rickshaw would needs about 5.93 kWh of extra energy from the grid and the nonsolar rickshaw 9.22

kWh. This means that about 3.26 kWh was supplemented by the solar panels, which corresponds to a reduction of 35% of the energy consumed by the solar rickshaw compared to the nonsolar rickshaw.

While for a cloudy day shown in 8, the figure reveals that the battery cannot suddenly start to store some amount of energy on the battery due to atmospheric conditions which causes the performance of the solar panels to drastically decrease, as will be discussed in the next section. Thus, the contribution of the solar panels is such that it only contributes to plus 12 km in the vehicle range.

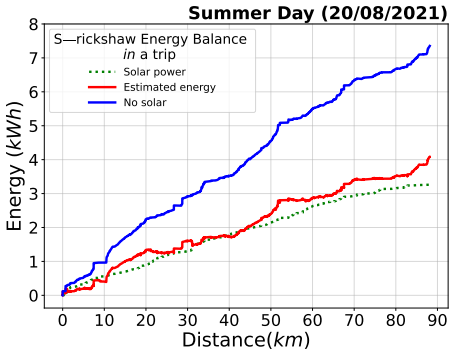

FIG. 7: Vehicle energy consumption estimation for a sunny day.

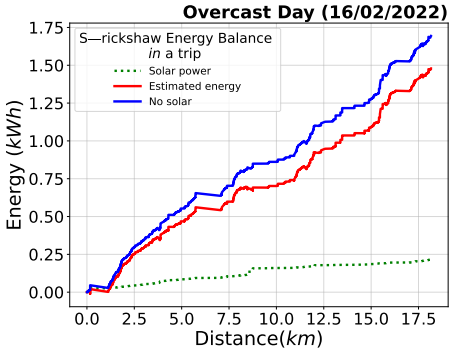

FIG. 8: Vehicle energy consumption estimation for a cloudy day.

VI. SOLAR BENEFITS

As seen in section V, the performance analysis gives an overall picture of the benefits of the proposed system. Some of this benefits are often categorized into driver, and economical benefits [21]. Both benefits are due to reduced energy consumption during the trip. In this section we present a detailed analysis of the aforementioned benefits provided by the solar rickshaw.

A. Driver Benefits

The two main driver benefits of adding solar panels to the rickshaw's roof for its charging are the range extension and the reduction of the cost of charging from the grid. The daily solar range extension may be calculated applying equation 10 below, where E_{rated} is the nominal capacity of the battery and E_{use} denotes the total energy used by the vehicle, here expressed in terms of kWh / 100 km.

$$D_{\max}\left[\frac{\text{km}}{\text{day}}\right] = \frac{E_{\text{rated}}\,[\text{kWh}]}{E_{\text{use}}\left[\frac{\text{kWh/100km}}{\text{day}}\right]} \times 100. \qquad (10)$$

Figure 9 shows the daily solar range extension for all the day of data collected. The results show that the maximum range was obtained on a clear sunny day in mid August, as expected. This indicates that more than 50% of the total daily distance traveled by the vehicle was provided by solar energy. However, the minimum range was reached in mid-October where the shading factors are more evident. In addition, it has also shown that average daily solar energy range extension is fairly 16 km, this is to be expected because the solar energy is highly variable throughout the day.

On the other hand, the second wise benefit is the reduced charging cost from the grid as represented in figure 10 for the same days. This improvement is in the same magnitude of solar range extension described above, which is to be expected because the price of buying electricity from the grid was considered to be constant and equal to 0.23 €/kWh.

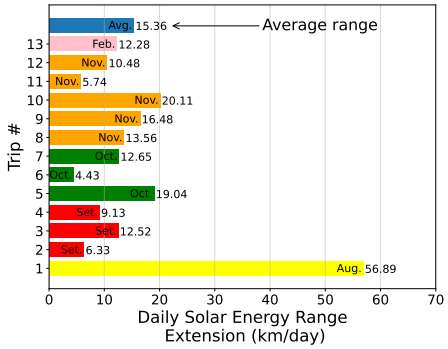

FIG. 9: Daily solar range extension for different days of data acquisition.

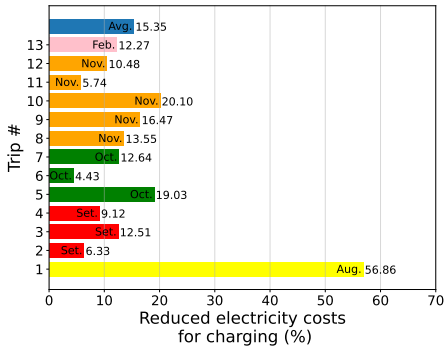

FIG. 10: Solar rickshaw effect on daily rickshaw charging. For comparison purposes, the total electricity cost for charging the nonsolar rickshaw is approximately $C_{ns} = 3.16$ €.

1. *Environmental Conditions*

Fig. 11 shows the efficiency of the solar panels over the day. Looking at the graph, one can immediately

see the effect of temperature on the performance of the module, i.e., when the cell temperature rise well above the ambient temperature, the efficiency of the module tends to decreases due to the low power generated. It was also calculated the relative error relatively to the expected maximum efficiency under STC, as can be seen in the figure (y-3 axis, red line).

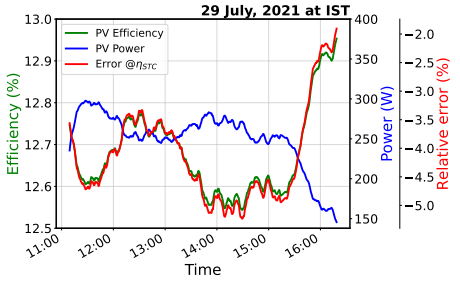

FIG. 11: Average photovoltaic panel efficiency over the day.

B. Economic Analysis

The success of any technology is quantified by its economic prospects. To access the economic feasibility of the proposed system, we will use two economic indicators. (i) Return on Investment (ROI) and (ii) the payback period (PP). ROI is a performance measure that is used to evaluate the additional profit generated due to certain benefits and is widely used across finance to compare different scenarios for an investment to profit. It can be calculated according to equation 11, where the value in the numerator corresponds to the total net benefit of investment, that is, the difference between the revenue and the investment cost during the system's lifetime.

$$ROI\ (\%) = \frac{G_{total} - C_{inv}}{C_{inv}} \times 100. \tag{11}$$

The cost of investment of the system can be estimated by applying a simple linear cost function, as represented in equation 12, where the first term corresponds to the price due to the photovoltaic module power; c_p is the cost of photovoltaic panel (€) and P_{PVp} is the total nominal photovoltaic panel installed capacity (kW), and the remaining terms correspond to the price owed to mounting, installation and maintenance costs, respectively. The total investment cost of the system was estimated for two different scenarios based on the current commercial prices for silicon solar modules [23]. The mounting cost (c_{mount}) with fuses and wires is estimated as 80 €. The installation cost (c_{inst}) was assumed to be 12% of the total cost of the system, found equal to 37.2 € and 26.54 €, respectively.

$$C_{inv}\ (€) = c_p P_{PVp} + c_{mount} + c_{inst} + c_{main} \tag{12}$$

The total maintenance cost for the entire life of the system was estimated using Eq. 13[24], where M_y is the yearly maintenance cost and taken to be approximately 2% of the initial cost of the system [24], i_r and d_r represent the inflation and discount rate, respectively, which is depending on the country's economy and for the case of Portugal found out to be 5.3% and 6% [25, 26]. The lifetime of the system was chosen based on the vehicle lifetime, which corresponds to the lifetime of the battery, which is equal to 6 years. However, since the solar panels has a warranted life of 20 years, 15 years was chosen here as a conservative value. So it is expected that at the end of the vehicle life-cycle this application can be transferred to another vehicle. All the system component costs are listed in table 12. For further calculations, the system's total cost was considered the average of the two already defined scenarios.

$$c_{main}\ (€) = M_y \times \left(\frac{1+i_r}{1+d_r}\right)\left(\frac{1-\left(\frac{1+i_r}{1+d_r}\right)^{T_{life}}}{1-\left(\frac{1+i_r}{1+d_r}\right)}\right) \tag{13}$$

Lastly, as said above the gain of investment is derived from the reduction in the energy consumption of the vehicle during trips. This gain can be calculated using equation 14, where C_{ele} is the electricity price and taken to be 0.23 €/kWh [27].

$$\begin{aligned} G_{\text{total}}\ (€) = {} & E_{\text{EV, non-solarEV}}(\text{kWh/km}) \times \\ & D_{\max}(\text{km/day}) \times C_{\text{ele}}(€/\text{kWh}) \\ & \times 365.25/4 \times T_{\text{life}}(\text{years}) \end{aligned} \tag{14}$$

In Figure 11 there can be seen the result of the estimated ROI during the system's lifetime. It is possible to see that when the vehicle was driven in the low solar radiation areas, i.e., from Autumn to Winter, ROI presented a very low value and even negative ($\sim -21\%$), as one should expected. Although, when the vehicle was driven in the high solar radiation area (typical sunny days), ROI presented a positive value and equal to 615%, which corresponds to a gain of approximately 7.15 times the initial investment cost. This is to be expected because as said previously the more solar radiation available the more solar energy range extension is expected to be achieved. It can also be seen the average ROI for all the day of the data collection, showing a positive value and 92%, which can be translated into a gain of 1.93 times the investment cost.

Another benefit is the amount of grid electricity saved, as represented in figure 13. The results reveal that a total of 10750 kWh of electricity can be saved from the grid on typical sunny days, which represents fairly to 44 € at each 4 months during the summer. Since this vehicle is mostly used to transport tourists during summer days where greater benefits are expected, the rest of the analysis are made considering this assumption.

The payback period of the investment refers to the length of time it takes to completely recover the cost of an investment. It is calculated according to the following equation [28], where t is the last year with negative cumulative cash flow, C_t is the cumulative

TABLE III: Cost of investment per components considered.

Component	High price	Low price	Note/Reference
PV Price c_p(€)	230.0	141.2	High and low estimation costs based on 0.33 €/W and 0.2 €/W [23]. Adding a tax rate of 7%.
Mounting cost c_{mount}(€)	80	80	
Subcomponents cost (€)	310	221.2	Summation of previous components
Installation cost c_{inst}(€)	37.2	26.54	12% of sub-components cost
Maintenance cost c_{main}	98.82	70.45	Equation (13)
Total cost C_{inv} (€)	407.8	281.3	Resulting in a mean total cost value equal to 382 €

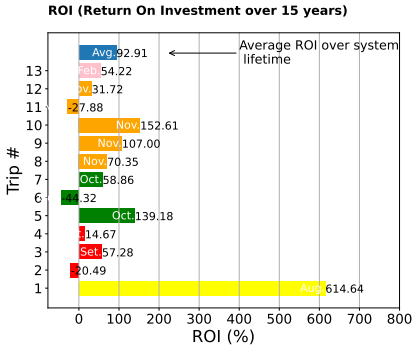

FIG. 12: Return On Investment over the system's lifetime considered.

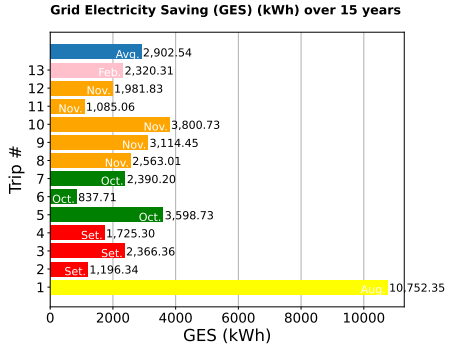

FIG. 13: Amount of the saving of grid electricity over the system's lifetime considered.

cash flow at year t (absolute value) and C_{t+1} is the cumulative cash flow at year $t+1$.

$$\text{Payback Period} = t + \frac{C_t}{C_{t+1}} \tag{15}$$

Based on the input parameters from table III, the payback period of the proposed solar rickshaw was found out to be approximately 5 years and the resultant trend can be seen in figure 14. The plot starts with a negative cash flow resulting from the capital investment to build the solar rickshaw. Over the years, the payback adds up and progress towards the positive side of cash flow. This means that after 5 years for the implementation of this system, the driver practically gets some amount of energy for free.

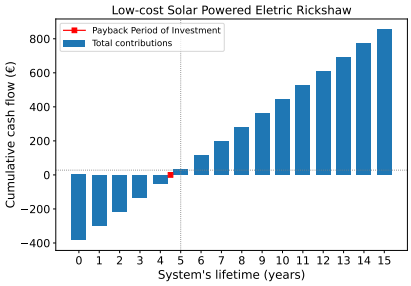

FIG. 14: Representation of he net cash flow during the proposed system's lifetime, which demonstrates a 10 years of recovery time after its installation.

VII. BATTERY SELECTION

The ultimately goal of this thesis is to select a new battery technology for the built solar rickshaw. As seen in previous sections for a typical sunny day, the solar panels on average can cover up to 35% of the energy consumed in the vehicle, which results in an average vehicle range of 0.087 kWh/km, which corresponds to 8.7 kWh/100 km. This represents to 35% increase in the range of the vehicle, relatively to the range provided by the manufacturer. Therefore, due to the seasonal nature of the vehicle, the new battery pack estimation can be taken practically to the limited of a similar reduction in the energy capacity of the batteries. The characteristics of the new proposed battery pack can be seen in table IV.

TABLE IV: Comparison between the actual battery pack in the vehicle [29] and the new battery pack proposed [30].

Parameter	$LiFePO_4$	New pack
Nominal Voltage	76.8 V	76.8 V
Capacity	180 Ah	120 Ah
Mass	135 kg	63.12 kg
Energy density	102 Wh/kg	164 Wh/kg
Cost per pack	186 €	132 €

VIII. CONCLUSIONS

Considering that the present Master's Thesis project had the objective of optimizing the process of charging electric rickshaw batteries with onboard photovoltaics with the purpose of demonstrating its usability based on a daily history of journeys deems the endeavor successful. Our results have shown that for a typical sunny day in the midseason, three solar panels of 220 W each with a conversion efficiency of 13.2%, solar power can cover up to 35% of the energy consumed in the vehicle. With this proposed system, an increase in autonomy of 56 km was achieved, relatively to the range provided by the manufacturer. On the other hand, for a typical winter day with the same solar power, an autonomy of 12 km is possible to be achieved. which indicates that this increment in the autonomy is sufficient to justify its use. Furthermore, the economic analysis of the proposed system predicted a ROI of 185% throughout the vehicle's lifetime of 6 years and a payback period of 5 years after the implementation of the system. Based on this result, a new battery pack was selected. It should be noted that, owing to the seasonal nature of the vehicle, where greater consumption is expected on sunny days due to its tourist characteristics, these savings can be taken practically to the limited of a similar reduction in the energy capacity of the batteries. This reduction in battery capacity leads to the reduction of 8% in vehicle weight.

[1] European Comission. Roadmap to a single europoean transport area - towards a competitive and resource efficient system. 2011.

[2] European Comission. Paris agreement. 2015.

[3] Matteo Muratori, Marcus Alexander, Doug Arent, Morgan Bazilian, Pierpaolo Cazzola, Ercan M Dede, John Farrell, Chris Gearhart, David Greene, Alan Jenn, Matthew Keyser, Timothy Lipman, Sreekant Narumanchi, Ahmad Pesaran, Ramteen Sioshansi, Emilia Suomalainen, Gil Tal, Kevin Walkowicz, and Jacob Ward. The rise of electric vehicles—2020 status and future expectations. *Progress in Energy*, 3(2):022002, mar 2021.

[4] International Energy Agency. *Global EV Outlook 2021*, 2021.

[5] Priscilla Mulhall, Srdjan M. Lukic, Sanjaka G. Wirasingha, Young-Joo Lee, and Ali Emadi. Solar/battery electric auto rickshaw three-wheeler. *2009 IEEE Vehicle Power and Propulsion Conference*, pages 153–159, 2009.

[6] Hannah Ritchie, Max Roser and Pablo Rosado. Energy. *Our World in Data*, 2020. https://ourworldindata.org/energy.

[7] Max Roser Hannah Ritchie and Pablo Rosado. Solar pv module prices. *Our World in Data*, 2019. https://ourworldindata.org/energy.

[8] Colin Cochrane, Tariq Muneer, and Bashabi Fraser. Design of an electrically powered rickshaw, for use in india. *Energies*, 12(17), 2019.

[9] Malik Sameeullah and Sunita Chandel. Design and analysis of solar electric rickshaw: A green transport model. In *2016 International Conference on Energy Efficient Technologies for Sustainability (ICEETS)*, pages 206–211, 2016.

[10] Sono Motors. Sion electric car. 2020. https://sonomotors.com/en/sion/.

[11] Lightyear one. Always charging in the sun. Longest range. Most sustainable. The electric car that charges itself with sunlight. https://lightyear.one/company.

[12] Felipe Andreolli Sell. O universo tuk tuk em lisboa: territorialidades, "drivers" e consumidores. Master's thesis, Instituto de Geografia e Ordenamento do Território (IGOT), 2019.

[13] David Neto. Trip and history-based range prediction for a light powered vehicle based on real-world data. Master's thesis, Instituto Superior Tecnico, 2020.

[14] Cedric De Cauwer, Joeri Van Mierlo, and Thierry Coosemans. Energy consumption prediction for electric vehicles based on real-world data. *Energies*, 8(8):8573–8593, 2015.

[15] Zonggen Yi and Peter H. Bauer. Adaptive multiresolution energy consumption prediction for electric vehicles. *IEEE Transactions on Vehicular Technology*, 66(11):10515–10525, 2017.

[16] Lino Guzella and Antonio Sciarretta. *Vehicle Propulsion Systems: Introduction to Modeling and Optimization*. Springer Berlin Heidelberg New York, 3 edition, 2013.

[17] M.C. Alonso García and J.L. Balenzategui. Estimation of photovoltaic module yearly temperature and performance based on nominal operation cell temperature calculations. *Renewable Energy*, 29(12):1997–2010, 2004.

[18] Gabi Friesen, Diego Pavanello, and Alessandro Virtuani. Overview of temperature coefficients of different thin film photovoltaic technologies. 2010.

[19] E-Tuk Factory. e-Tuk Limo GT Brochure. 2020.

[20] OpenTopography. Shuttle radar topography mission (srtm) global. 2013. Online; accessed 10 March 2022.

[21] Muhammad Hosnee Mobarak, Rafael N. Kleiman, and Jennifer Bauman. Solar-charged electric vehicles: A comprehensive analysis of grid, driver, and environmental benefits. *IEEE Transactions on Transportation Electrification*, 7(2):579–603, 2021.

[22] A. Sripakagorn C. Chaiyamanon and N. Noomwongs. Dynamic modeling of electric tuk-tuk for predicting energy consumption in bangkok driving condition. *SAE Technical Papers*, 2013.

[23] PV insitights. Grid the World. 2017. Accessed: 2022-05-27.

[24] Mahmoud Abdelhamid, Srikanth Pilla, Rajendra Singh, Imtiaz Haque, and Zoran Filipi. A comprehensive optimized model for on-board solar photovoltaic system for plug-in electric vehicles: energy and economic impacts: On-board solar photovoltaic system for plug-in electric vehicles. *International Journal of Energy Research*, 40, 09 2016.

[25] Trading Economics. Portugal Inflation Rate. 2022. [Online; accessed 5-Jun-2022].

[26] Y Charts. Portugal Long Term Interest Rate. 2022. [Online; accessed 5-Jun-2022].

[27] Global Petrol Prices. Portugal preços da electricidade. 2022. [Online; accessed 5-Jun-2022].

[28] Catarina G. B. Ventura. Techno-economic analysis of charging posts to be installed in a hub for electric vehicles. Master's thesis, Instituto Superior Tecnico, 2019.

[29] GWL. Calb 180ah lifepo4 battery datasheet.

[30] GWL. Calb 135ah lifepo4 battery datasheet.